Original Research - Emerging Technology

GMP-level adipose stem cells combined with computer-aided manufacturing to reconstruct mandibular ameloblastoma resection defects: Experience with three cases

Access this article online
Website: www.amsjournal.com
DOI: 10.4103/2231-0746.119216
Quick Response Code:

Jan Wolff[1,2], George K. Sándor[1,3], Aimo Miettinen[2], Veikko J. Tuovinen[4], Bettina Mannerström[1], Mimmi Patrikoski[1], Susanna Miettinen[1]

[1]Institute of Biomedical Technology, University of Tampere, [2]Department of Eye, Ear and Oral Diseases, Tampere University Hospital, Tampere, [3]Department of Oral and Maxillofacial Surgery, University of Oulu, Oulu, [4]Department of Oral and Maxillofacial Surgery, Central Hospital of Central Finland Health Care District, Jyväskylä, Finland

Address for correspondence:
Prof. George K. Sándor, Institute of Biomedical Technology, University of Tampere, Biokatu 12 Krs 6, 33520 Tampere, Finland.
E-mail: george.sandor@uta.fi

ABSTRACT

Background: The current management of large mandibular resection defects involves harvesting of autogenous bone grafts and repeated bending of generic reconstruction plates. However, the major disadvantage of harvesting large autogenous bone grafts is donor site morbidity and the major drawback of repeated reconstruction plate bending is plate fracture and difficulty in reproducing complex facial contours. The aim of this study was to describe reconstruction of three mandibular ameloblastoma resection defects using tissue engineered constructs of beta-tricalcium phosphate (β-TCP) granules, recombinant human bone morphogenetic protein-2 (rhBMP-2), and Good Manufacturing Practice (GMP) level autologous adipose stem cells (ASCs) with progressively increasing usage of computer-aided manufacturing (CAM) technology. **Materials and Methods:** Patients' three-dimensional (3D) images were used in three consecutive patients to plan and reverse-engineer patient-specific saw guides and reconstruction plates using computer-aided additive manufacturing. Adipose tissue was harvested from the anterior abdominal walls of three patients before resection. ASCs were expanded *ex vivo* over 3 weeks and seeded onto a β-TCP scaffold with rhBMP-2. Constructs were implanted into patient resection defects together with rapid prototyped reconstruction plates. **Results:** All three cases used one step *in situ* bone formation without the need for an ectopic bone formation step or vascularized flaps. In two of the three patients, dental implants were placed 10 and 14 months following reconstruction, allowing harvesting of bone cores from the regenerated mandibular defects. Histological examination and *in vitro* analysis of cell viability and cell surface markers were performed and prosthodontic rehabilitation was completed. **Discussion:** Constructs with ASCs, β-TCP scaffolds, and rhBMP-2 can be used to reconstruct a variety of large mandibular defects, together with rapid prototyped reconstruction hardware which supports placement of dental implants.

Keywords: Adipose-derived stem cells, beta-tricalcium phosphate, bone morphogenetic protein, computer-aided design

INTRODUCTION

While many strategies have been proposed for the management of mandibular bony defects following avulsive trauma or ablative surgery,[1] autogenous bone grafts are considered the "gold standard" for reconstructive bone surgery[2] to the present day.

Small mandibular defects (<4-6 cm) are often treated with nonvascularized corticocancellous grafts harvested from the anterior or posterior iliac crest.[2,3] Larger defects are commonly treated with vascularized fibula grafts[2,4,5] which offer a long pedicle length, wide vessel diameter, and the possibility to incorporate skin, muscle and bicortical bone components when such tissues are required.[6] However, the use of vascularized

autologous tissue grafts requires healthy donor tissues and vessels. Morbidity of large bone graft harvesting is a deterrent to fibular bone flap use,[7-10] therefore less morbid treatment strategies would be advantageous.[11]

Bone tissue engineering regenerates osseous tissue by combining biomaterials, bioactive molecules, and stem cells.[11-14] One reliable source of stem cells for bone regeneration is autologous fat tissue which provides an abundant amount of adipose stem cells (ASCs).[15,16] ASCs are capable of multiple lineage differentiation to chondrocyte, adipocyte, and osteoblast pathways.[15] The harvesting of fat tissue is simple and causes less morbidity when compared to standard bone harvesting techniques.[15-19] One other advantage of ASCs over human bone marrow stromal/stem cells (BMSCs) is that BMSCs are present in low frequency in the bone marrow, whereas ASCs can be retrieved in high numbers from adipose tissue and can easily be expanded *in vitro*.[14,20] Using the tissue engineering model,[12] it has been possible to harvest autogenous ASCs from patients and use the cells to seed a resorbable scaffold.[21,22]

Biomaterials of various types and forms can serve as scaffolds in bone tissue engineering, including granular forms and solid blocks. Although they have no load bearing ability, compared to blocks, granular forms present more surface area for cellularization. Granules are more quickly incorporated into host tissues than block forms which remodel more slowly.[23] Granules have a tendency to migrate within a wound and must be retained at the site of intended implantation by a containment mesh made of either titanium or a resorbable biomaterial. Granular calcium phosphate ceramics and related biomaterials such as hydroxyapatite possess macro- and microstructural properties that make them useful biomaterials in tissue engineering. Such properties affect cell attachment, survival, signaling, growth, and propagation.[23,24] While some inorganic ceramics may also bind directly to bone,[25] the surfaces of other biomaterials may affect differentiation of stem cells to osteoblasts.[26]

Growth factors such as bone morphogenetic proteins (BMP) have recently been added to constructs in order to promote osteoinductive properties.[27-29]

Although major segments of human mandibular defects have been reconstructed with constructs containing growth factors such as recombinant human BMP-7 (rhBMP-7),[27,30] reports regarding cell-seeded constructs are still few in number.[22,24,31-36] While there has been much laboratory study of possible techniques,[37-39] most clinical reports describe the occasional single case success.[22,31-36]

One deficiency in planning complex reconstructive surgery using either autologous bone or tissue engineered constructs is the inability to predictably produce complex facial contours using commercially available reconstruction plates and meshes. Commercially available reconstruction plates are supplied as generic sizes and shapes being designed on the basis of the 'average' patient. These reconstruction plates are often made from titanium and are supplied as straight or slightly contoured metal plates with predrilled holes for retention by screws. The surgeon may spend considerable time during surgery bending and shaping the plate to fit the contour of the patient's bone. Titanium reconstruction plates currently used for mandibular defects are subject to both over-bending and a lack of passive fitting which may eventually lead to fatigue fractures.[40]

One solution to this problem is to use computer-guided surgical planning and additive manufacturing technology to produce a passive fitting implant designed for patient specific anatomical needs.[41] Progress in medical imaging and continued incremental increases in computer processing power available for both three-dimensional patient data acquisition and subsequent image processing make it possible for clinicians to diagnose, more accurately plan, simulate, and treat their patients.[42]

To date the most common use of additive manufacturing has been the fabrication of patient-specific skull models for preoperative planning. These skull models are fabricated using patient specific imaging data in the form of Digital Imaging and Communications in Medicine (DICOM) files, which are then converted into stereolithography (STL) files, and used to print the patient specific skull models. The use of such three-dimensional (3D) medical models helps surgeons to plan, simulate the planned operation, and manually pre-bend commercially available reconstruction plates.[43] Recent developments in the area of additive manufacturing allow the prefabrication of patient specific, customized, reconstruction plates using the patient's DICOM data. The advantages of rapid prototyped reconstruction plates are that they do not require intraoperative bending and offer improved passive fitting. In light of possible material failure, better structural designs may be developed according to individual anatomy at the design stage.

The aim of this study was to reconstruct segmental mandibular defects resulting from ameloblastoma resection in a small series of non-radiated patients using a tissue engineered construct consisting of beta-tricalcium phosphate (β-TCP) granules, rhBMP-2 in conjunction with ASCs. Additionally, the authors sought to gradually incorporate a 3D computer-aided surgical workflow, from diagnosis to surgical treatment, in order to provide patients with complimentary hardware to help restore mandibular ameloblastoma resection defects.

MATERIALS AND METHODS

A total of three patients with recurrent ameloblastomas requiring segmental mandibular resection were included in this study. There were two males and one female with an average age of 49.3 years ranging from 43 to 55 years [Table 1]. The planned mandibular segmental resection defects ranged from 6.0 to 10.0 cm in length with an average defect size of 8.2 cm [Figures 1-3]. There was no history of radiation therapy in any of the three cases. Two patients were in good health. Case 3 was congenitally blind. Case 1 had been previously presented in a single case report[36] and was now included with further follow-up as part of this series of three patients.

The combination of ASCs and biomaterials are considered to be an advanced therapy combined medicinal product according to the regulations of the European Medicines Agency. The treatment was carried out with the approval of FIMEA, the Finnish

Table 1: Patient details of cases with mandibular defects treated with good manufacturing practice level adipose stem cells

Patient Number	Demographics Gender/Age	Defect Size	Mandibular Defect Site	Ossification Site	BMP-2 dose	Scaffold β-TCP	Implanted ASCs/cc	Containment Mesh	Dental Implants Placed	Failed Dental Implants	Follow-up
1	M 55	10.0 cm	Chin	in situ	12mg	granules 40 cc	10,000,000	Titanium	6 fixtures	1 fixture	43 months
2	F 50	8.5 cm	Left Ramus and Body	in situ	12mg	granules 40 cc	16,000,000	Titanium	1 fixture	None	21 months
3	M 43	6.0 cm	Left Body	in situ	12mg	granules 40 cc	4,720,000	Titanium	None	None	19 months

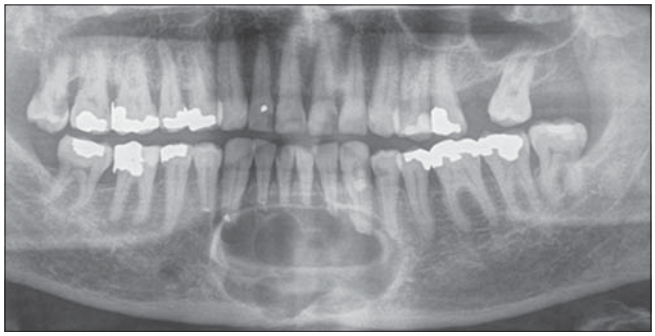

Figure 1: Preoperative panoramic radiograph of case 1 with recurrent ameloblastoma at symphyseal region of anterior mandible

Figure 2: Preoperative panoramic radiograph of case 2 with recurrent ameloblastoma at left body and ramus of mandible. Note the proximity of the lesion to the most distal mandibular dental implant

Figure 3: Preoperative panoramic radiograph of case 3 with recurrent ameloblastoma at the left body of the mandible

Medicines Agency under hospital exemption of patient specific treatment (Dnro 615/11.01.06./2010). The approval to use ASCs for research purposes was granted by the Ethics Committee of the Pirkanmaa Hospital District, Tampere, Finland (R03058) within the ethical principles of the Declaration of Helsinki. Prior to surgery, the patients were thoroughly informed about the procedures, which they approved and to which they gave their written consent.

Planning and reverse engineering

Prior to planning the operation 3D stereolithographic medical skull models (Planmeca, Helsinki, Finland) were fabricated using the patients' preoperative computed tomography (CT) noncompressed DICOM voxel-based data set. The medical skull models allowed visualization and assessment of the planned resection defects and were also used to pre-bend commercially available reconstruction plates and titanium meshes for later use in the reconstructions.

The acquired patient DICOM data sets were also imported into Pro Model Romexis virtual surgical planning software program (Planmeca, Helsinki, Finland) after which patient specific 3D preoperative planning was performed [Figures 4-6]. The novel Pro Model Romexis software program was capable of performing virtual mandibular resections, manipulate bony segments, and mirror the anatomy of the unaffected side [Figure 7]. The calculated virtual reconstructions were then converted into STL software file format to generate the information needed to fabricate custom-made medical skull models, saw guides, and reconstruction plates. The custom-made saw guides were produced using an additive manufactured process with a Z printer 450 (Z Corporation Rock Hill, SC, USA), a commercial printer which creates objects by curing composite powder and ink jetting. The reconstruction plates were manufactured using titanium powder and selective laser sintering (SLS) technology. This method of additive manufacturing uses a laser beam to fuse and solidify titanium powder. Successive layers of powder are deposited and raster scanned creating a highly accurate medical-grade titanium (Ti6A14V ELI) custom reconstruction plate.

ASCs isolation and cell culturing

Three to four weeks prior to mandibular resection, approximately 50-100 ml of subcutaneous adipose tissue was harvested from the anterior abdominal wall [Figure 8] to be used for *ex vivo* tissue culturing and future autologous reimplantation. Additionally, 50-60 ml of autologous serum was obtained for the expansion of autologous stem cells.

Patient specific autologous ASCs from cases 1, 2, and 3 were isolated and expanded *in vitro* in Good Manufacturing

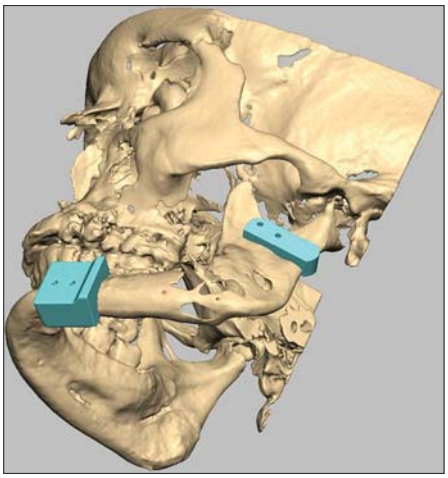

Figure 4: Virtual preoperative planning using Romexis software in case 2. The picture illustrates saw guides precisely over the resection position

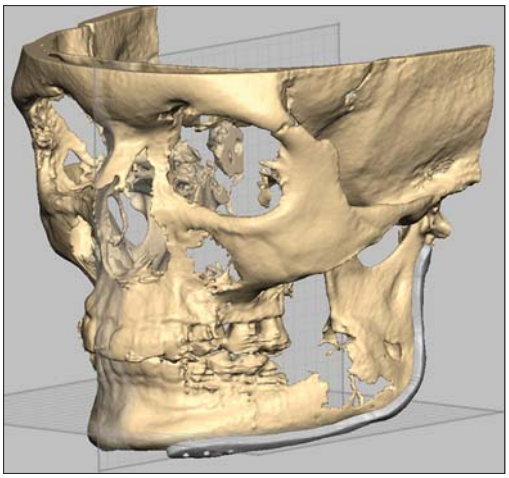

Figure 5: The computer generated image of case 2 shows the reconstruction plate over the area planned for resection

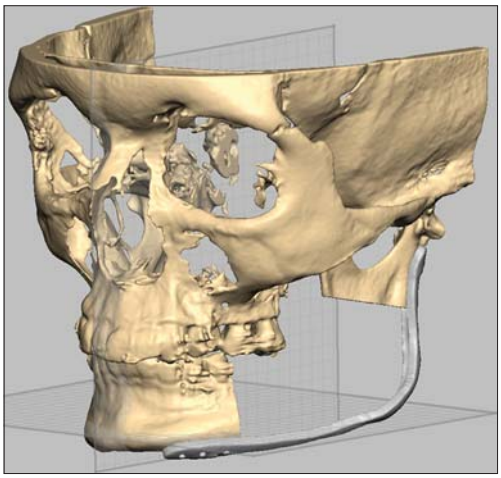

Figure 6: This computer generated virtual planning image of case 2 shows the resection and shape of reconstruction plate based on the mirrored healthy side of mandible

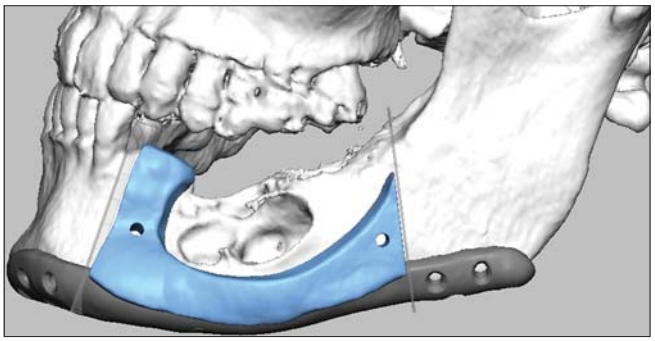

Figure 7: This computer generated virtual planning image of case 3 shows the resection jig in place with the shape of reconstruction plate based on the mirrored healthy side of mandible

Figure 8: Three weeks prior to mandibular resection, 50-60 ml of autologous serum and approximately 50-100 ml of subcutaneous adipose tissue was harvested from the anterior abdominal wall for *ex vivo* tissue culturing and autologous reimplantation

Practice (GMP) clean room according to standard operating procedures at Regea Cell and Tissue Center, Institute of Biomedical Technology, University of Tampere and BioMediTech. Isolation and expansion procedures were performed as reported previously with minor modifications.[14,21] The adipose tissue was minced and digested with recombinant collagenase NB 6 (Invitrogen, Paisley, Scotland, United Kingdom; GMP grade; SERVA Electrophoresis GmbH, Heidelberg, Germany).

The isolated cells were expanded for 21 days in basal media (BM) containing Dulbecco's modified Eagle medium/F-12 (Gibco Invitrogen, Paisley, Scotland, United Kingdom) with 15% of autologous serum, without antibiotics, and were subsequently passaged on confluency, detached mechanically with a cell scraper, and prepared for cell transplantation. This yielded an average of 10,240,000 cells (range 4,720,000-16,000,000) of passages three to four, for each of the three patients [Table 1]. These cells were combined with 40 mL of β-TCP granules (Chronos1, porosity 60%, granule size 1.4-2.8 mm; Synthes, Oberdorf, Switzerland) 48 h before the operation to allow cell attachment to the biomaterial. Prior to combining the cells with β-TCP, the material was incubated for 48 h in basal medium (BM) containing 12 mg rhBMP-2 (InductOS, Wyeth Europa, Berkshire, UK). Following the incubation, the BM containing rhBMP-2 was discarded.

Cell sterility and endotoxins were tested by Biovian Ltd. (Turku, Finland) according to methods described in the European Pharmacopoeia (Council of Europe, Strasbourg, France). The cells tested negative for mycoplasma contamination as determined by a mycoplasma polymerase chain reaction (PCR) kit (VenorGem; Minerva Biolabs GmbH, Berlin, Germany). The genomic integrity of hASCs was verified using a standard chromosome G-banding method. Karyotypic evaluation was performed as an outsourcing service in Medix Laboratories Ltd. (Espoo, Finland).

Cell attachment to the material and the cell viability were studied using live/dead staining prior to the cell transplantation operation. Briefly, the cell-biomaterial combination was incubated with a mixture of CellTracker™ green (5-chloromethylfluorescein diacetate (CMFDA, Molecular Probes, Eugene, Oregon, USA) and ethidium homodimer (EH-1; Molecular Probes). The viable cells (green fluorescence) and dead cells (red fluorescence) were detected with a fluorescence microscope [Figure 9].

ASCs were further expanded *in vitro* and the immunophenotype of the cells was analyzed by flow cytometry (FACSAria®, BDBiosciences, Erembodegem, Belgium). Monoclonal antibodies (MAb) against CD11a-allophycocyanin (APC), CD80-phycoerythrin (PE), CD86-PE, CD105-PE (R&D Systems Inc., Minneapolis, MN, USA), CD3-PE, CD14-phycoerythrin-cyanine (PECy7), CD19-PECy7, CD45RO-APC, CD54-fluorescein isothiocyanate (FITC), CD73-PE, CD90-APC (BD Biosciences), and CD34-APC, HLA-DR-PE (Immunotools GmbH, Friesoythe, Germany) were used [Table 2]. Analysis was performed on 10,000 cells per sample and unstained cell samples were used to compensate for the background autofluorescence levels.

Due to the limited amount of autologous serum for the subsequent *in vitro* analyses, basic medium supplemented with 10% human serum type AB (Lonza Bioscience Rockland, Romeoville, IL, USA), and 1% antibiotics (100 U/ml penicillin, 0.1 mg/ml streptomycin; Invitrogen) were used.

Table 2: Surface marker expression of adipose stem cells by flow cytometry (FACS) of 10,000 cells analyzed. Data are presented as average and standard deviation obtained from all three patient samples

ASC FACS results

Surface Protein Abbreviation	Surface protein description	Average	Standard deviation
CD3	T-cell coreceptor	5.8	2.6
CD11a	ITGAL, integrin alpha L	0.6	0.4
CD14	Monocyte differentiation antigen	21.5	9.0
CD19	B lymphocyte surface antigen B4	9.9	5.0
CD34	Sialomucin-like adhesion molecule	1.7	2.1
CD45	Leucocyte common antigen	3.1	1.8
CD54	ICAM-1, Intercellular adhesion molecule 1	20.8	1.4
CD73	Ecto 5′ nucleotidase	99.9	0.1
CD80	B lymphocyte activation antigen B7-1	8.9	1.3
CD86	B lymphocyte activation antigen B7-2	22.0	4.7
CD90	Thy-1	98.5	2.3
CD105	SH-2, endoglin	99.9	0.2
HLA-DR	MHC class II cell surface receptor	2.7	2.7

Multipotency of the ASCs was analyzed by adipogenic, osteogenic, and chondrogenic differentiation. The differentiation capacity was evaluated after 14 days of differentiation induction in adipogenic, osteogenic or chondrogenic medium versus cells cultured in control medium. Briefly, for the *in vitro* osteogenic differentiation analyses, ASCs were maintained on a 12-well plate at a density of 2.5×10^3 cells/cm^2 in osteogenic media (OM), containing BM supplemented with 250 mM L-ascorbic acid 2-phosphate (Sigma Aldrich, St Louis MO, USA), 10 mM β-glycerophosphate (Sigma Aldrich) and 5 nM dexamethasone (Sigma Aldrich). The cultures were subsequently analysed by alkaline phosphatase staining (ALP). The cell cultures were fixed with a 4% paraformaldehyde solution (PFA) and stained with alkaline phosphatase according to the Sigma Aldrich Procedure No. 86 (#86R-1KT) to detect early osteogenesis.

For the *in vitro* adipogenic differentiation analyses, surplus ASCs were maintained on a 12-well plate at a density of 2×10^4 cells/cm^2 in adipogenic media containing BM supplemented with 33 μM biotin (Sigma Aldrich), 1 μM dexamethasone (Sigma Aldrich), 100 nM insulin (Life Technologies), and 17 μM pantothenate (Fluka, Buchs, Switzerland). In addition, 250 μM isobutylmethylxanthine (IBMX; Sigma) was used for the first 24 h of adipogenic induction. Cell cultures were fixed with 4% PFA and stained with 0.5% Oil Red O solution (Sigma Aldrich) for detection of oil droplets. For the chondrogenic differentiation, 1×10^5 cells were seeded on 24-well plates in a 10 μl volume as micromasses, and were allowed to adhere for 3 h in + 37°C prior to the addition chondrogenic medium; BM supplemented with 1% ITS + 1 (Sigma Aldrich), 50 μM ascorbic acid (Sigma Aldrich), 55 μM sodium pyruvate (Life Technologies), 23 μM L-proline (Sigma Aldrich), and 10 ng/ml TGF-β (Sigma Aldrich). The micromass pellets were fixed in 4% PFA, embedded in paraffin and sectioned at 5 μm thickness. Alcian blue solution was used to detect cartilaginous matrix glycosaminoglycans, with nuclear Fast Red (Biocare Medical, Concord, MA, USA) as counterstain.

Ameloblastoma resection protocol

Before segmental mandibulectomy all three patients were placed into maxillomandibular fixation unilaterally using fixation screws and elastic bands to maintain condylar position. An extraoral submental incision in case 1 or submandibular approaches in cases 2 and 3 were used to expose the parasymphysis or the body and ramus of the mandible on the defect side. A commercially available 2.4 mm generic reconstruction plate was used in cases 1 and 2 (Synthes, Obersdorf, Switzerland) and additive manufactured 2.4 mm custom-made titanium reconstruction plates (Planmeca, Helsinki, Finland) were attached to the affected hemimandible and fixed with 2.4 mm titanium screws in cases 2 and 3. After fixating the reconstruction plate, virtually simulated osteotomy lines from the preoperative planning were easily located intraoperatively with help of prefabricated saw guides [Figures 9-12] that were fixed on top of the already screw retained rapid prototyped reconstruction plate.

The entire tumor with a margin of healthy tissue was excised as planned in each case [Figure 13]. The healthy ends of the resected mandibles were maintained in their correct orientations with the attached hardware. The defects resulting from ameloblastoma resection were immediately reconstructed using a preformed

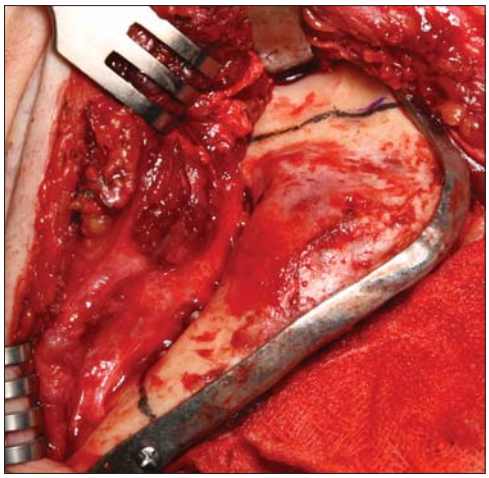

Figure 9: Intraoperative photograph of case 2 showing reconstruction plate applied to mandible with resection lines transferred from resection jig onto the mandible

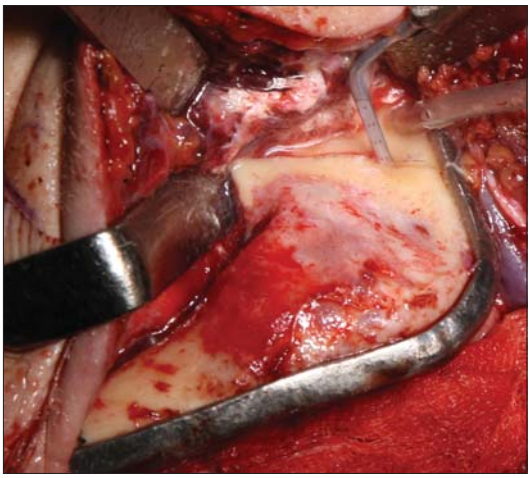

Figure 10: Intraoperative photograph of case 2 with superior resection line transferred from computer generated plan being cut with a piezo-surgical tip

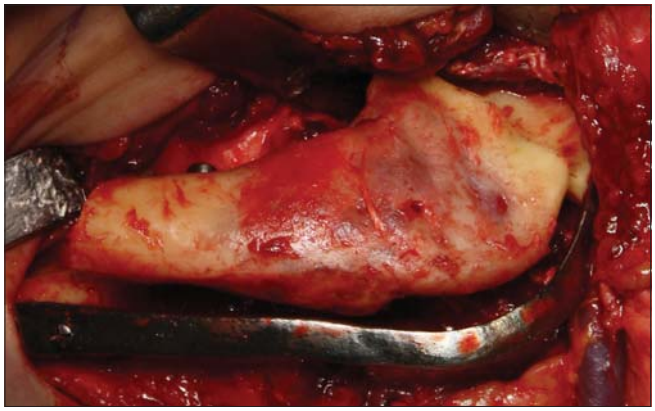

Figure 11: Intraoperative photograph of case 2 showing both resection lines completed and resected fragment being lifted from wound without the need to remove the reconstruction plate. The reconstruction plate maintains correct orientations of the mesial and distal resection stumps

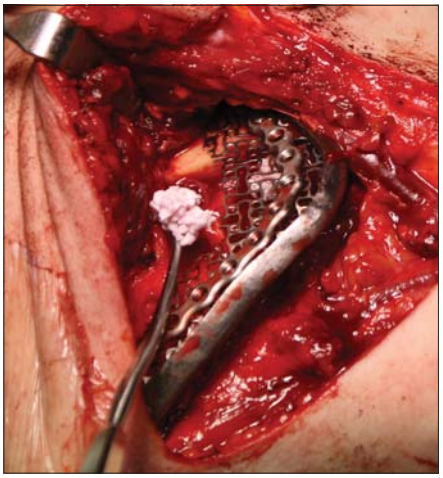

Figure 12: Intraoperative photograph of case 2 with ASC containing granules of β-TCP and rhBMP-2 being packed beneath the titanium containment mesh

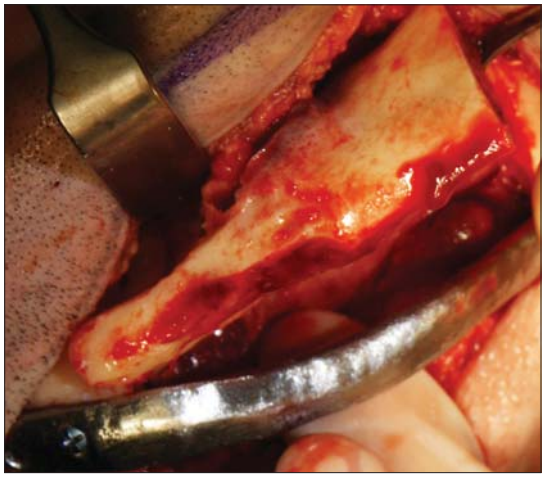

Figure 13: Intraoperative photograph of case 3 with reconstruction plate applied and resected fragment being lifted from the wound without the need to remove the reconstruction plate which was situated at the lower border of mandible. The reconstruction plate maintains correct orientations of the mesial and distal resection stumps

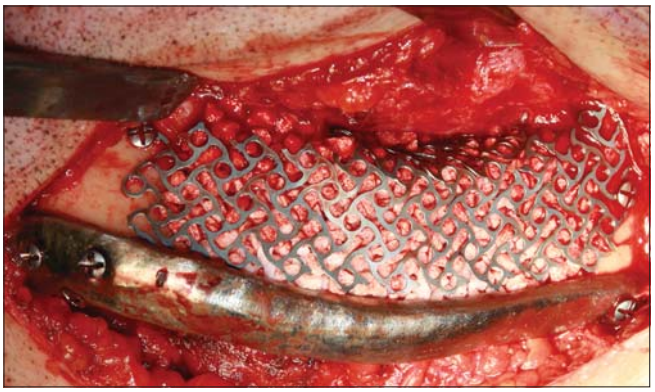

Figure 14: Intraoperative photograph of case 3 showing the titanium containment mesh in place and its underlying space filled with granular scaffold of β-TCP and rhBMP-2

custom-made titanium mesh fixated onto the ends of the mandibular defects using 1.5 mm titanium screws. The space beneath the mesh was filled with rhBMP-2 and ASCs seeded β-TCP granules [Figures 14-16]. To avoid exposure of the titanium mesh to the oral cavity, the final height of the titanium mesh was kept lower than that of the resected mandibular bone. Routine layered wound closure was performed.

Dental implant operation protocol

After uneventful healing of 10 months in case 1 and 14 months in case 2, both patients underwent dental implant placement in the reconstructed and healed defects [Figures 17-20]. Case 3 chose not to have dental implant treatment. In both case 1 and 2 the intraoperative clinical evaluation of the augmented defect sites revealed healthy non-inflamed soft tissues and dense hard tissue. After exposing the grafted sites, 6 Straumann SLActive implants were placed into case 1 and one Straumann SLActive bone level implant was placed into case 2 (Straumann AG, Basel, Switzerland) [Table 1]. Bone cores were retrieved during the implant insertion procedure from the bone necessary for removal at the implant osteotomy sites. The retrieved bone cores were processed to obtain histological material for further tests on cell viability, proliferation, and osteogenic differentiation in cases 1 and 2.

The cells from the bone core samples were allowed to sprout and proliferate in BM *in vitro* and were subsequently analyzed by flow cytometry. MAb against surface proteins ALP-APC, CD105-PE, BMPR1-FITC, FGFR2-APC, FGFR3-PE, TGFβ1-PE, VEGFR1-PE, VEGFR2 -Peridinin chlorophyll protein (PerCP), VEGFR3-APC (R&D Systems Inc., Minneapolis, MN, USA), CD45RO-APC, CD90-APC (BD Biosciences), and CD34-APC, HLA-DR-PE (Immunotools GmbH, Friesoythe, Germany) were used. Further, intracellular markers VEGF-PE, latent TGFβ-PE and TWIST-1-FITC (R&D Systems) were used according to the manufacturer's protocols. The analysis was performed as described for ASCs above.

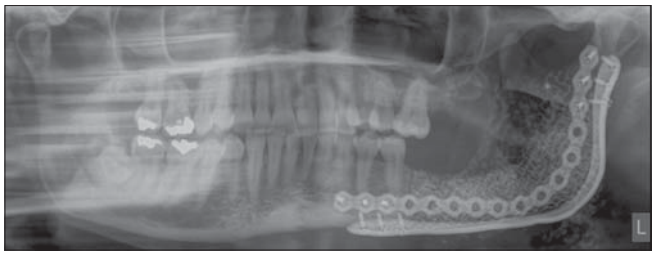

Figure 15: Immediate postoperative panoramic radiograph of case 2 showing reconstruction plates, titanium containment mesh, and granular scaffold in place on the ramus, angle, and body regions of the left mandible

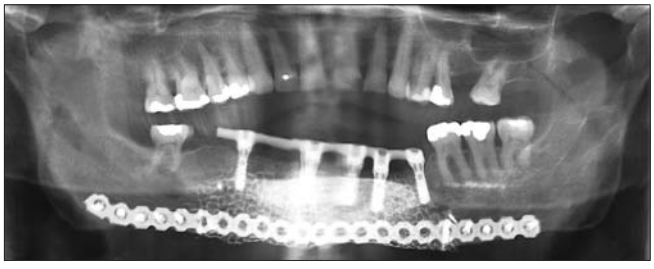

Figure 17: Panoramic radiograph taken 3.0 years after insertion of dental implants into the reconstructed symphysis of Case 1

RESULTS

The reconstruction of the three mandibular defects with GMP level ASCs was successful in bridging the large defects averaging 8.2 cm (range 6.0-10.0 cm) with uneventful healing [Table 1]. Two of the three patients opted for reconstruction with dental implants [Figures 17-20]. There were seven fixtures placed in two patients and six (86%) successfully osseointegrated and were loaded prosthodontically. The three patients have been under follow-up for an average of 28 months following their cell based mandibular reconstructions (range: 19-43 months).

In two of the three patients, the preoperative virtual designs were transferred as planned to the mandibular resection sites. The reconstruction plates were capable of maintaining the anatomical spatial relation of the ends of the resected mandible and there was excellent passive fit of the plates at their respective resection sites.

Laboratory results

ASCs recovered from the adipose tissue proliferated in the autologous serum and cell morphology was spindle-shaped [Figure 21]. The live/dead staining showed that viable and adherent ASC were transplanted with the β-TCP granules into the patient [Figure 22]. Osteogenic, adipogenic, and chondrogenic differentiation was evident in differentiated samples showing the multipotent nature of ASCs [Figures 23-25].

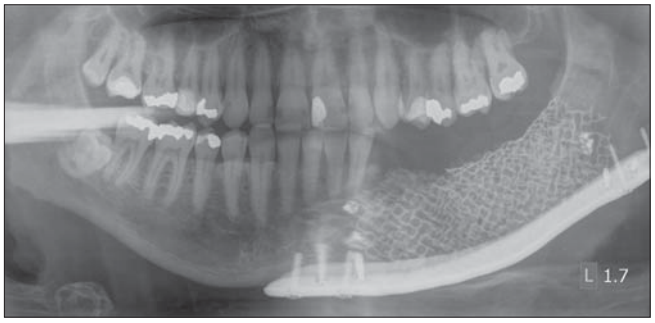

Figure 16: Immediate postoperative panoramic radiograph of case 3 showing reconstruction plates, titanium containment mesh, and granular scaffold in place on the body and angle region of the left mandible

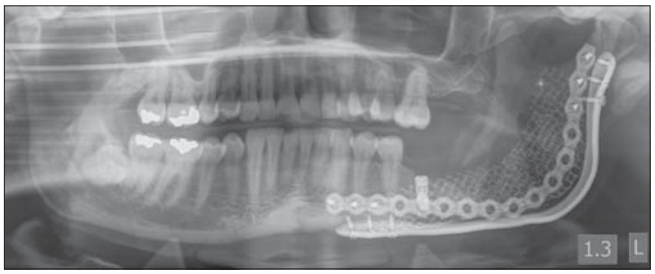

Figure 18: Immediate post dental implant insertion panoramic radiograph from Case 2 showing dental implant placed into the reconstructed alveolus of the left posterior mandible

The flow cytometry results of ASCs [Tables 2 and 3] showed strong expression of mesenchymal markers CD73, CD90, and CD105; moderate expression of CD14, CD19, CD54, CD80, and CD86; and low or no expression of CD3, CD11a, CD34, CD45, and HLA-DR. However, the immunophenotype showed patient variability; especially in CD3, CD14, CD19, and HLA-DR; a tendency that has also been reported previously[14] [Table 2].

The re-entry and bone drilling necessitated by the placement of dental implants or removal of parts of the edges of almost exposed titanium mesh after 10 and 14 months healing, allowed the opportunity to biopsy the healing construct and by obtaining cores at the implant osteotomy sites.

The flow cytometric analysis on cells derived from bone samples [Tables 4 and 5] showed strong expression of mesenchymal markers CD90, CD105, and TWIST-1; moderate expression of FGFR3 and intracellular VEGF; low expression of CD34, CD45, FGFR2, ALP, BMPR1, VEGFR1, VEGFR3, and latent TGFβ; and no expression of TGFβ1, HLA-DR, and VEGFR2. As seen in the ASCs, the surface marker expression showed patient variability, particularly in CD34, CD45, FGFR2, FGFR3, VEGFR1, and intracellular VEGF [Table 2].

Histologic analysis of the recovered bone cores revealed signs of bone formation and remodeling. The β-TCP granules were interconnected by bridges of vital newly formed bone [Figures 26 and 27].

DISCUSSION

The degree of involvement of computer-aided design (CAD) and additive manufacturing progressively increased over the time in which the three cases were treated. In the first case an additive manufactured medical skull model was used preoperatively to guide pre-bending of patient specific hardware including a generic reconstruction plate and titanium mesh. In the two cases that followed, custom-made reconstruction plates requiring no bending as well as resection jigs were made using CAD software, and the practitioners became more confident in using these tools. For example, in case 1 only a pre-bent generic reconstruction plate guided by the contours of the stereolithic skull was used. In case 2, the custom-made reconstruction plate made with CAD was used together with a pre-bent generic plate as the surgeons were not confident in the load bearing ability of solely the custom-made plate. The generic plate was omitted as redundant in case 3, once a finite element analysis model[44-46] specific for these custom-made

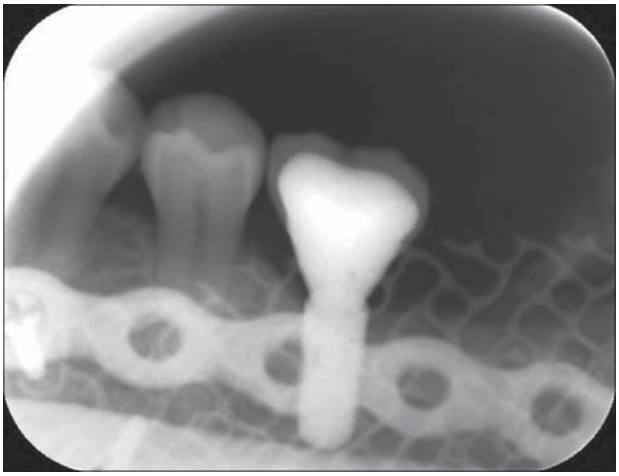

Figure 19: Periapical radiograph showing osseointegrated dental implant in Case 2 loaded with prosthetic crown

Figure 20: Intraoral view of dental implant in Case 2 and its restored crown on the mandibular left first molar tooth

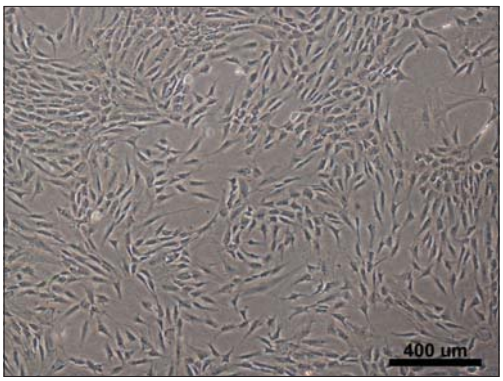

Figure 21: Case 2 *in vitro* microscopic images of adipose stem cells (ASCs) in culture 7 days post isolation

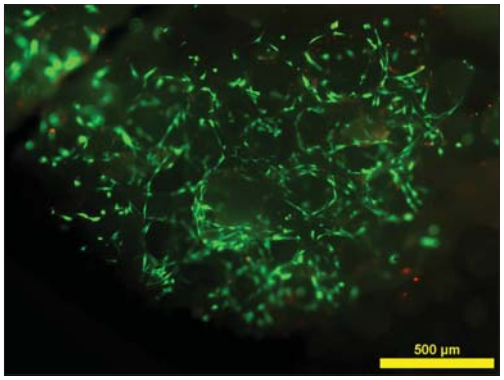

Figure 22: Fluorescence microscope image of live/dead staining of ASCs on biomaterial, with live cells staining green and dead cells staining red, showing cell adhesion to the biomaterial and cell viability

Table 3: Column diagram from flow cytometry data of adipose stem cells (ASCs). Columns illustrate mean surface marker expression levels with standard deviation error bars of all three patient samples

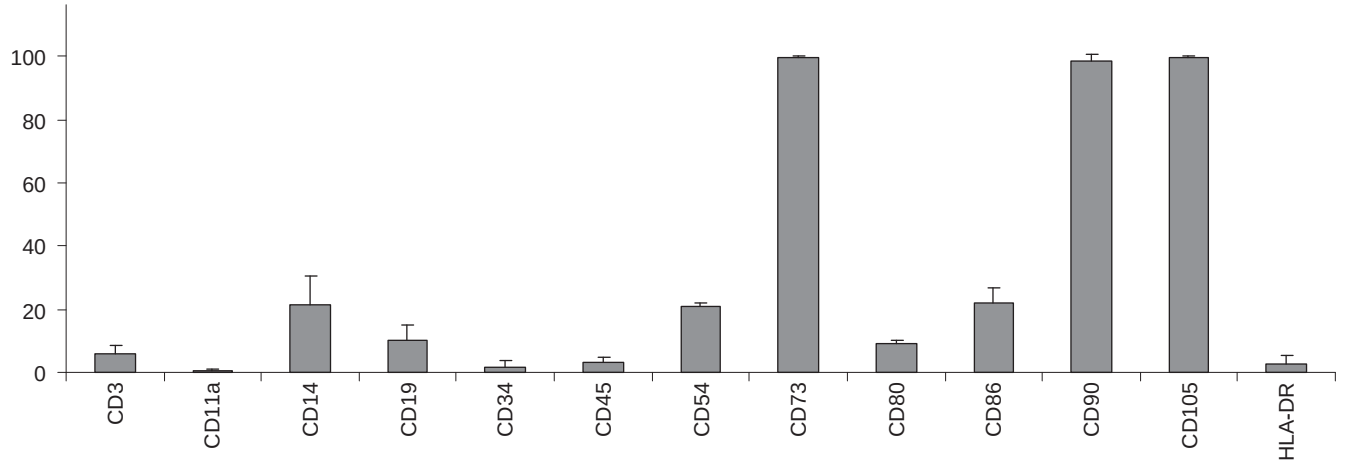

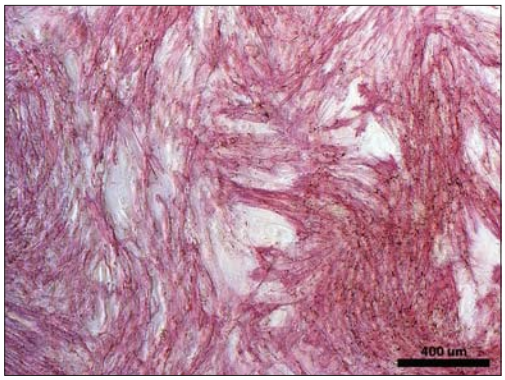

Figure 23: Alkaline phosphatase staining (red) on osteogenic differentiation cultures of ASCs

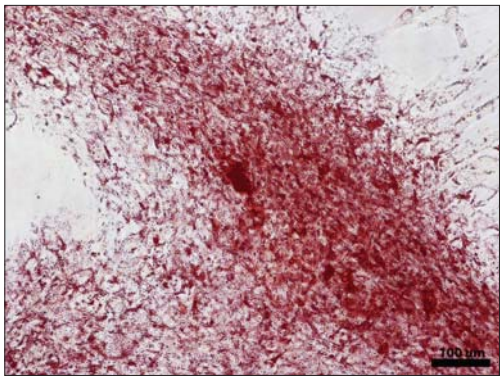

Figure 24: Oil red O staining confirming adipose differentiation of ASCs cultured in monolayer

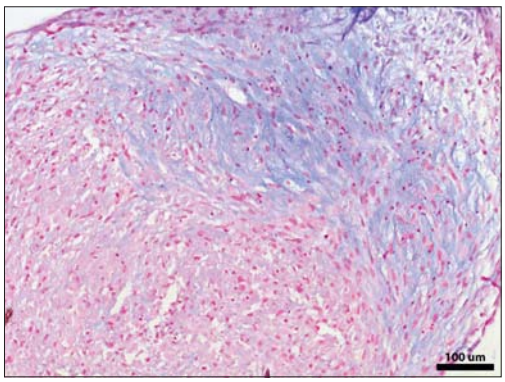

Figure 25: Alcian blue staining confirming chondrogenic differentiation of ASCs cultured in micromass culture format

plates became available to better predict the loading and stress distribution of the computer designed hardware. The accuracy of such CAD-computer aided manufacturing (CAD-CAM) based reconstructions using virtual surgical planning have recently been determined.[47]

This report describes successful mandibular reconstruction in a series of three patients using the approach of *in situ* ossification with GMP level ASCs[36] as one non-morbid source of autogenous mesenchymal stem cells (MSCs). In order to appreciate fully the cell source used, thorough *in vitro* analysis was implemented [Figures 21-25].

In this cohort, there was individual variability in cell numbers available for implantation from passages three to four as the average cell number was 10,240,000 cells with a range of 4,720,000-16,000,000 cells. The characterization data of the ASCs expanded in autologous serum correspond to previous results for ASCs,[36,48] with positive expression of certain markers substantiating the mesenchymal origin of cells and negative expression of other markers suggesting the hematopoietic and angiogenic origin of cells.[48,49] Nevertheless, very few reports have been published regarding the surface marker expression of ASC expanded in autologous serum.[14,22,36,50] For the markers CD11a, CD54, CD80, and CD86 no results have previously been reported on ASCs cultured in human serum. The multipotency analyzes verified the stem cell capacities of the ASCs of all three patients. To our knowledge, the marker profile on culture expanded osteoblasts from core bone samples have not been reported previously. The surface

Table 4: Surface marker expression of osteoblasts determined by flow cytometry (FACS) of 10,000 cells analyzed. Data are presented as average and standard deviation obtained from all three patient samples

Osteoblast FACS results			
Surface Protein Abbreviation	**Surface protein description**	**Average**	**Standard deviation**
CD34	Sialomucin-like adhesion molecule	6.2	6.6
CD45	Leucocyte common antigen	7.2	7.0
CD90	Thy-1	100.0	0.0
CD105	SH-2, endoglin	99.8	0.3
FGFR2	Fibroblast growth factor receptor 2	6.2	7.0
FGFR3	Fibroblast growth factor receptor 3	11.0	11.8
HLA-DR	MHC class II cell surface receptor	0.4	0.0
ALP	Alkaline phosphatase	1.0	0.8
BMPR1	Bone morphogenetic protein receptor type II	1.3	0.6
TGFβ1	Transforming growth factor beta 1	0.6	0.1
VEGFR1	Vascular endothelial growth factor receptor-1	2.3	2.7
VEGFR2	Vascular endothelial growth factor receptor-2	0.3	0.1
VEGFR3	Vascular endothelial growth factor receptor-3	1.4	0.3
VEGF	Vascular endothelial growth factor	39.7	55.5
LatentTGFβ	Latent transforming growth factor beta 1	4.6	2.6
TWIST-1	Twist-related protein 1	86.0	15.8

markers show strong expression of mesenchymal markers as well as moderate to low expression of several angiogenic and osteogenic markers.

The *in vitro* and *in vivo* bone forming capacity of ASCs in combination with various scaffold materials, including β-TCP, has been reported by our group and others.[14,22,36,51,52] Furthermore, the use of osteogenic growth factor rhBMP-2 might have facilitated ossification.[51,52] Nevertheless, contradictory reports have also been published, including reports of BMP-2 possibly not promoting osteogenic differentiation of human MSCs.[53-55] However, the transplanted ASCs produce cytokines and chemokines that act as homing signals for endogenous stem cells and progenitor cells to the site of injury.[56] The factors secreted by the ASCs and the osteoconductivity of β-TCP act synergistically towards producing a well-ossified construct.[56]

Titanium hardware was chosen over resorbable materials because at the time the cases were treated, the track record of resorbable hardware for major mandibular reconstruction was still lacking. Since the authors decided to use granules rather than a solid block, a containment mesh was required to house the scaffold. The authors were concerned that with the thin soft tissue coverage

Table 5: Column diagram from flow cytometry data of osteoblasts. Columns illustrate mean surface marker expression levels with standard deviation error bars of all three patient samples

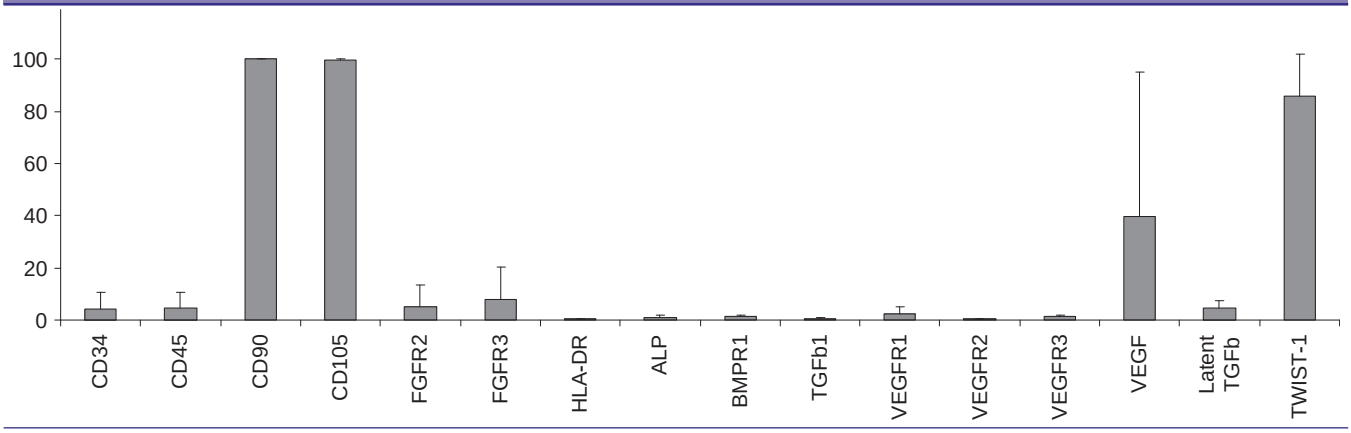

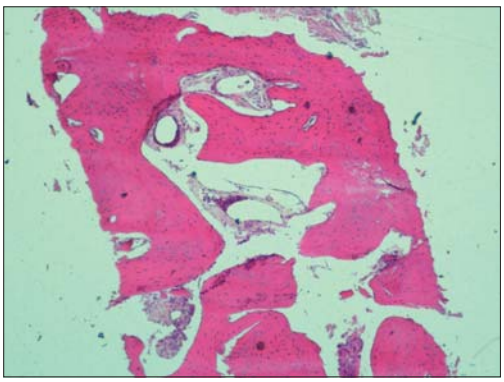

Figure 26: Hematoxylin and eosin stained section of bone from case 2 obtained from dental implant drilling site showing healthy bone (original magnification, ×200)

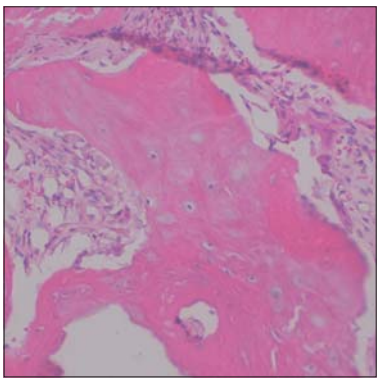

Figure 27: Hematoxylin and eosin stained section of bone from case 3 obtained from titanium mesh removal site showing healthy woven bone and areas of angiogenesis (original magnification, ×400)

of the mandibular alveolus, the wound might not tolerate the additional pH drop resulting from degradation of a resorbable polymer mesh containing polylactic acid.

Titanium mesh was problematic in all three cases with thin soft tissue coverage and each of the three patients required resection of the superior borders of the mesh. For this reason the authors would prefer to use a thin custom-made passive fitting resorbable mesh once a suitable tested version becomes available. The authors considered many resorbable scaffolds such as bioactive glass but chose β-TCP granules because of its more rapid resorption profile.[23-26] In the future, the authors could consider using scaffolds containing carriers which would release bioactive molecules such as growth factors and other drugs.

While both Warnke *et al*., 2004[33,34] and Mesimäki *et al*., 2009[22] have reported single cases of mandibular and maxillary defect reconstruction using bone marrow or adipose derived stem cells, the current three cases are unique. Both groups of previous authors used an ectopic muscle pouch site for bone induction.

The current three cases used the same type of GMP level autologous stem cells as did Mesimäki *et al*.,[22] but there was no need for an ectopic bone formation step. Instead the construct was put directly into its final recipient bed from the outset. This obviated the need for an ectopic bone formation site and this protocol has been called *in situ* bone formation.[32,36]

Preparation of the recipient site by maximizing the contact of the construct with well vascularized muscle is most important with *in situ* bone formation.[36] There was no history of prior radiation therapy in these three cases. Unlike the present cases, the patient reported by Mesimäki *et al*., had a very complicated wound with pre-existing oronasal and oroantral fistulae, requiring soft tissue coverage on two sides.[22] In such complex cases requiring soft tissues in addition to bone, or in cases where there has been prior radiation therapy, these authors feel that it is best to use ectopic ossification as the preferred method over *in situ* bone formation.

The components of the constructs used in these reconstructions are thought to act synergistically. The ASCs serve as a reservoir of functional stem cells. The rhBMP-2 functions as a signaling molecule inducing osteogenic differentiation within its half-life. The β-TCP bone substitute acts as a scaffold to support osteogenesis and remodeling of bone. The sequence of these events is hopefully accelerated by the collective presence of these three entities.

One major drawbacks of this novel treatment was increased costs to the Finnish healthcare system. The GMP level ASC laboratory preparation costs were 10,000 Euros or approximately 12,000 US dollars for each patient. The cost of the use of planning software and production of additive manufactured saw guides and reconstruction plates was 1,000 euros or 1,200 US dollars more than using commercially available generic reconstruction hardware.

CONCLUSION

Rapid prototyped saw guides and reconstruction plates combined with tissue engineered constructs containing osteogenic cells, such as GMP level ASCs, osteoinductive factors like rhBMP-2 in combination with a synthetic osteoconductive matrix β-TCP granules, can be used to reconstruct large ameloblastoma resection defects of the mandible. *In situ* bone formation is an attractive alternative for such large bony defects without a history of radiation therapy or without complicated wounds which require vascularized soft tissue transfers with an ectopic bone formation protocol.

ACKNOWLEDGMENTS

The authors wish to acknowledge Sari Kalliokoski, Anna-MaijaHonkala, MiiaJuntunen, TiiaTallinen, Hanna Kankkonen, and AnikkaHakamäki for their valuable contributions which made this work possible. This study has been financially supported by EVO (9L100), the Competitive Research Funding of Tampere University Hospital and the Finnish Funding Agency for Technology and Innovation (TEKES).

REFERENCES

1. Bianchi B, Ferri A, Ferrari S, Leporati M, Copelli C, Ferri T, *et al*. Mandibular resection and reconstruction in the management of extensive ameloblastoma. J Oral Maxillofac Surg 2013;71:528-37.
2. Pogrel MA, Podlesh S, Anthony JP, Alexander J. A comparison of vascularized and nonvascularized bone grafts for reconstruction of mandibular continuity defects. J Oral Maxillofac Surg 1997;55:1200-6.
3. Goh BT, Lee S, Tideman H, Stoelinga PJ. Mandibular reconstruction in adults: A review. Int J Oral Maxillofac Surg 2008;37:597-605.
4. Schliephake H. Revascularized tissue transfer for the repair of complex midfacial defects in oncologic patients. J Oral Maxillofac Surg 2000;58:1212-8.
5. Hidalgo DA. Fibula free flap: A new method of mandible reconstruction. Plast Reconstr Surg 1989;84:71-9.
6. Thankappan K, Trivedi NP, Subash P, Pullara SK, Peter S, Kuriakose MA, *et al*. Three-dimensional computed tomography-based contouring of a free fibula bone graft for mandibular reconstruction. J Oral Maxillofac Surg 2008;66:2185-92.
7. Sándor GK, Nish IA, Carmichael RP. Comparison of conventional surgery with motorized trephine in bone harvest from the anterior iliac crest. Oral Surg Oral Med Oral Pathol Oral Radiol Endod 2003;95:150-5.
8. Ling XF, Peng X. What is the price to pay for a freefibula flap? A systematic review of donor-site morbidity following free fibula flap surgery. Plast Reconstr Surg 2012;129:657-74.
9. Sieg P, Taner C, Hakim SG, Jacobsen HC. Long-term evaluation of donor site morbidity after freefibula transfer. Br J Oral Maxillofac Surg 2010;48:267-70.
10. Nathan SS, Athanasian E, Boland PJ, Healey JH. Valgus ankle deformity after vascularized fibular reconstruction for oncologic disease. Ann Surg Oncol 2009;16:1938-45.
11. Gimbel M, Ashley RK, Sisodia M, Gabbay JS, Wasson KL, Heller J, *et al*. Repair of alveolar cleft defects: Reduced morbidity with bone marrow stem cells in a resorbable matrix. J Craniofac Surg 2007;18:895-901.
12. Langer R, Vacanti JP. Tissue engineering. Science 1993;260:920-6.
13. Sándor GK, Suuronen R. Combining adipose-derived stem cells, resorbable scaffolds and growth factors: An overview of tissue engineering. J Can Dent Assoc 2008;74:167-70.
14. Thesleff T, Lehtimäki K, Niskakangas T, Mannerström B, Miettinen S, Suuronen R, *et al*. Cranioplasty with adipose-derived stem cells and biomaterial: A novel method for cranial reconstruction. Neurosurgery 2011;68:1535-40.
15. Gimble JM, Zvonic S, Floyd ZE, Kassem M, Nuttall ME. Playing with bone and fat. J Cell Biochem 2006;98:251-66.
16. Chamberlain G, Fox J, Ashton B, Middleton J. Concise review: Mesenchymal stem cells: Their phenotype, differentiation capacity, immunologic features, and potential for homing. Stem Cells 2007;25:2739-49.
17. Song L, Tuan RS. Transdifferentiation potential of human mesenchymal stem cells derived from bone marrow. FASEB J 2004;18:980-2.

18. Pittenger MF, MacKay AM, Beck SC, Jaiswal RK, Douglas R, Mosca JD, *et al*. Multilineage potential of adult human mesenchymal stem cells. Science 1999;284:143-7.
19. Wolf NS, Penn PE, Rao D, McKee MD. Intraclonal plasticity for bone, smooth muscle, and adipocytes lineages in bone marrow stroma fibroblastoid cells. Exp Cell Res 2003;290:346-57.
20. Zimmermann CE, Gierloff M, Hedderich J, Acil Y, Wiltfang J, Terhyden H. Survival of transplanted rat bone marrow-derived osteogenic stem cells *in vivo*. Tissue Eng Part A 2011;17:1147-56.
21. Lindroos B, Suuronen R, Miettinen S. The potential of adipose stem cells in regenerative medicine. Stem Cell Rev 2011;7:269-91.
22. Mesimäki K, Lindroos B, Törnwall J, Mauno J, Lindqvist C, Kontio R, *et al*. Novel maxillary reconstruction with ectopic bone formation by GMP adipose stem cells. Int J Oral Maxillofac Surg 2009;38:201-9.
23. Leong KF, Cheah CM, Chua CK. Solid freeform fabrication of three-dimensional scaffolds for engineering replacement tissues and organs. Biomaterials 2003;24:2363-78.
24. Schliephake H, Zghoul N, Jäger V, van Griensven M, Zeichen J, Gellinsky M, *et al*. Effect of seeding technique and scaffold material on bone formation in tissue-engineered constructs. J Biomed Mater Res A 2009;90:429-37.
25. Haimi S, Moimas L, Pirhonen E, Lindroos B, Huhtala H, Räty S, *et al*. Calcium phosphate surface treatment of bioactive glass causes a delay in early osteogenic differentiation of adipose stem cells. J Biomed Mater Res A 2009;91:540-7.
26. Hammerle CH, Olah AJ, Schmid J, Flückiger L, Gogolewski S, Winkler JR, *et al*. The biological effect of natural bone mineral on bone neoformation on the rabbit skull. Clin Oral Implants Res 1997;8:198-207.
27. Clokie CM, Sándor GK. Reconstruction of 10 major mandibular defects using bioimplants containing BMP-7. J Can Dent Assoc 2008;74:67-72.
28. Cheng H, Jiang W, Phillips FM, Haydon RC, Peng Y, Zhou L, *et al*. Osteogenic activity of the fourteen types of human bone morphogenetic proteins. J Bone Joint Surg Am 2003;85-A:1544-52.
29. Barr T, McNamara AJ, Sándor GK, Clokie CM, Peel SA. Comparison of the osteoinductivity of bioimplants containing recombinant human bone morphogenetic proteins 2 (Infuse) and 7 (OP-1). Oral Surg Oral Med Oral Pathol Oral Radiol Endod 2010;109:531-40.
30. Moghadam HG, Urist MR, Sándor GK, Clokie CM. Successful mandibular reconstruction using a BMP bioimplant. J Craniofac Surg 2001;12:119-27.
31. Torroni A. Engineered bone grafts and bone flaps for maxillofacial defects: State of the art. J Oral Maxillofac Surg 2009;67:1121-7.
32. Khojasteh A, Behnia H, Dashti SG, Stevens M. Current trends in mesenchymal stem cell application in bone augmentation: A review of the literature. J Oral Maxillofac Surg 2012;70:972-82.
33. Warnke PH, Springer IN, Wiltfang J, Acil Y, Eufinger H, Wehmöller M, *et al*. Growth and transplantation of a custom vascularised bone graft in a man. Lancet 2004;364:766-70.
34. Warnke PH, Springer IN, Acil Y, Julga G, Wiltfang J, Ludwig K, *et al*. The mechanical integrity of *in vivo* engineered heterotopic bone. Biomaterials 2006;27:1081-7.
35. Behnia H, Khojasteh A, Soleimani M, Tehranchi A, Atashi A. Repair of alveolar cleft defect with mesenchymal stem cells and platelet derived growth factors: A preliminary report. J Craniomaxillofac Surg 2012;40:2-7.
36. Sándor GK, Tuovinen VJ, Wolff J, Patrikoski M, Jokinen J, Nieminen E, *et al*. Adipose stem cell (ASC) tissue-engineered construct used to treat large anterior mandibular defect: A case report and review of the clinical application of GMP-level ASCs for bone regeneration. J Oral Maxillofac Surg 2013;71:938-50.
37. Terheyden H, Knak C, Jepsen S, Palmie S, Rueger DR. Mandibular reconstruction with a prefabricated vascularized bone graft using recombinant human osteogenic protein-1: An experimental study in miniature pigs. Part I: Prefabrication. Int J Oral Maxillofac Surg 2001;30:373-9.
38. Terheyden H, Warnke P, Dunsche A, Jepsen S, Brenner W, Palmie S, *et al*. Mandibular reconstruction with prefabricated vascularized bone grafts using recombinant human osteogenic protein-1: An experimental study in miniature pigs. Part II: Transplantation. Int J Oral Maxillofac Surg 2001;30:469-78.
39. Terheyden H, Menzel C, Wang H, Springer IN, Rueger DR, Acil Y. Prefabrication of vascularized bone grafts using recombinant human osteogenic protein-1-part 3: Dosage of rhOP-1, the use of external and internal scaffolds. Int J Oral Maxillofac Surg 2004;33:164-72.
40. Kokemueller H, Spalthoff S, Nolff M, Tavassol F, Essig H, Stuehmer C, *et al*. Prefabrication of vascularized bioartificial bone grafts *in vivo* for segmental mandibular reconstruction: Experimental pilot study in sheep and first clinical application. Int J Oral Maxfac Surg 2010;39:379-87.
41. Arias-Gallo J, Maremonti P, González-Otero T, Gómez-García E, Burgueño-García M, Chamorro Pons M, *et al*. Long term results of reconstruction plates in lateral mandibular defects. Revision of nine cases. Auris Nasus Larynx 2004;31:57-63.
42. Abou-ElFetouh A, Barakat A, Abdel-Ghany K. Computer-guided rapid-prototyped templates for segmental mandibular osteotomies: A preliminary report. Int J Med Robot 2011;7:187-92.
43. Christensen AM, Humphries SM. Role of rapid digital manufacture in planning and implementation of complex medical treatments. In: Gibson I, editor. Advanced Manufacturing Technology for Medical Applications. Sussex: John Wiley and Sons Ltd; 2006. p. 16.
44. McDonald JA, Ryall CJ, Wimpenny DI. Rapid Prototyping Casebook. London: Professional Engineering Publishing Stratasys; 2001. p. 260.
45. Bujtár P, Sándor GK, Bojtos A, Szűcs A, Barabás J. Finite element analysis of the human mandible at three developmental stages. Oral Surg Oral Med Oral Pathol Oral Radiol Endod 2010;110:301-9.
46. Bujtar P, Simonovics J, Váradi K, Sándor GK, Pan J, Avery CM. Refinements in osteotomy design to improve structural integrity: A finite element analysis study. Br J Oral Maxillofac Surg 2012.
47. Foley BD, Thayer WP, Honeybrook A, McKenna S, Press S. Mandibular reconstruction using computer-aided design and computer-aided manufacturing: An analysis of surgical results. J Oral Maxillofac Surg 2013;71:e111-9.
48. Strem BM, Hicok KC, Zhu M, Wulur I, Alfonso Z, Schreiber RE, *et al*. Multipotential differentiation of adipose tissue-derived stem cells. Keio J Med 2005;54:132-41.
49. Gimble J, Guilak F. Adipose-derived adult stem cells: Isolation, characterization, and differentiation potential. Cytotherapy 2003;5:362-9.
50. Shahdadfar A, Frønsdal K, Haug T, Reinholt FP, Brinchmann JE. *In vitro* expansion of human mesenchymal stem cells: Choice of serum is a determinant of cell proliferation, differentiation, gene expression, and transcriptome stability. Stem Cells 2005;23:1357-66.
51. Conejero JA, Lee JA, Parrett BM, Terry M, Wear-Maggitti K, Grant RT, *et al*. Repair of palatal bone defects using osteogenically differentiated fat-derived stem cells. Plast Reconstr Surg 2006;117:857-63.
52. Dragoo JL, Lieberman JR, Lee RS, Deugarte DA, Lee Y, Zuk PA, *et al*. Tissue-engineered bone from BMP-2-transducedstem cells derived from human fat. Plast Reconstr Surg 2005;115:1665-73.
53. Waselau M, Patrikoski M, Juntunen M, Kujala K, Kääriäinen M, Kuokkanen H, *et al*. Effects of bioactive glass S53P4 or betatricalcium phosphate and Bone Morphogenetic Proteins2 and bone morphogenetic protein7 on osteogenic differentiation of human adipose stem cells. J Tissue Eng 2012;3:114-26.
54. Tirkkonen L, Haimi S, Huttunen S, Wolf J, Pirhonen E, Sándor GK, *et al*. Osteogenic medium is superior to growth factors in differentiation of human adipose stem cells towards bone-forming cells in 3D culture. Eur Cell Mater 2013;25:144-58.
55. Kyllönen L, Haimi S, Mannerström B, Huhtala H, Rajala KM, Skottman H, Sndor GK *et al*. Effects of different serum conditions on osteogenic differentiation of human adipose stem cells *in vitro*. Stem Cell Res Ther 2013;4:17.
56. Prockop DJ. "Stemness" does not explain the repair of many tissues bymesenchymal stem/multi*poten*t stromalcells (MSCs). Clin Pharmacol Ther 2007;82:241-3.

Cite this article as: Wolff J, Sándor GK, Miettinen A, Tuovinen VJ, Mannerström B, Patrikoski M, *et al*. GMP-level adipose stem cells combined with computer-aided manufacturing to reconstruct mandibular ameloblastoma resection defects: Experience with three cases. Ann Maxillofac Surg 2013;3:114-25.

Source of Support: The Finnish Funding Agency for Technology and Innovation (TEKES) and the Competitive Research Funding of Tampere University Hospital, **Conflict of Interest**: None declared.